Journal of Applied Polymer Science

Highly Porous Catalytic Materials with Pd and Ionic Liquid Supported on Chitosan

Claire Jouannin,[1,2] Chloë Vincent,[1] Isabelle Dez,[2] Annie-Claude Gaumont,[2] Thierry Vincent,[1] Eric Guibal[1]

[1]Ecole des Mines d'Alès, Laboratoire Génie de l'Environnement Industriel, Interfaces Fonctionnalisées pour l'Environnement et la Sécurité, F-30319 ALES Cedex, France

[2]Laboratoire de Chimie Moléculaire et Thioorganique, UMR CNRS 6507, INC3M, FR 3038, ENSICAEN, Université de Caen, 14050 Caen, France

Correspondence to: C. Jouannin (E-mail: claire.jouannin@ensicaen.fr)

ABSTRACT: Chitosan was used to immobilize phosphonium-based ionic liquids, combined with silica particles, to prepare catalytic materials in the form of highly porous monoliths. These catalytic materials were studied for the hydrogenation of 4-nitroaniline into *p*-phenylenediamine in the presence of formic acid as hydrogen donor in a column reactor. Experimental conditions for the elaboration of the materials were evaluated by their impact on palladium sorption, on the structure of the materials, and on their catalytic efficiency. The concentration of chitosan in the initial solution and the size and concentration of silica particles had to be carefully chosen to elaborate homogeneous materials, with good mechanical resistance and stability in water. The chitosan characteristics and the type of ionic liquid immobilized in the material did not significantly affect the structure of the materials but proved to be crucial for their catalytic efficiency. Higher catalytic performances were obtained using materials prepared from chitosan of high-deacetylation degree and with Cyphos IL-101. © 2012 Wiley Periodicals, Inc. J. Appl. Polym. Sci. 000: 000–000, 2012

KEYWORDS: polysaccharides; catalysts; ionic liquids; porous materials; biomaterials

Received 3 April 2012; accepted 20 August 2012; published online
DOI: 10.1002/app.38501

INTRODUCTION

Catalysis is used in most industrial chemical processes. Heterogeneous catalysts or supported catalysts are mainly preferred for industrial applications as they allow an easy extraction of the product and an improved recovery of the catalyst for a potential recycling. However, heterogeneous catalysis presents some limitations due to the accessibility of active species and lower diffusion properties, leading to lower activity when compared with homogeneous catalysis. To overcome these limitations, supported ionic liquid catalysts (SILCs) were developed. A SILC consists in a layer of ionic liquid containing the homogeneous catalyst, immobilized at the surface of a solid support. The ionic liquid containing the catalyst behaves as a homogeneous phase with enhanced mass transfer properties and higher activity, while the immobilization on a porous support allows an easy separation of the product, potential recycling of the catalyst, and development for continuous processes.[1–3] The use of ionic liquids as a homogeneous phase for the catalyst benefits from their low volatility and their good solubility for organic complexes.[4,5] The SILCs were first developed on inorganic supports (such as SiO_2)[5,6] and more recently on biopolymer supports (such as alginates and chitosan).[7–10] To improve catalytic properties, the porous support should present a high surface area to enhance diffusion properties.[7,10–12] Moreover, the elaboration of SILCs gives an opportunity to develop continuous fixed-bed reactors.[6]

We recently reported the use of alginate as an immobilizing matrix for tetraalkyl phosphonium ionic liquids and palladium to elaborate catalytic materials in the form of highly porous monoliths (HPMs).[10,13] These catalytic materials presented a good catalytic efficiency for the hydrogenation of 4-nitroaniline (4-NA), with fast reaction kinetics, without palladium leaching. However, the influence of the support used in SILCs has previously been reported, highlighting the impact of the functionality of the biopolymer support (either amino for chitosan or carboxylic acid for alginate) on pallado-catalyzed Tsuji–Trost reactions.[8] Chitosan is a linear amino polysaccharide, composed of *β*-(1-4)-linked D-glucosamine and *N*-acetyl-D-glucosamine, obtained from the deacetylation of chitin, mostly extracted from the exoskeletons of crustacea. The degree of deacetylation and

Additional Supporting Information may be found in the online version of this article.

Table I. Characteristics of Chitosan Samples

Chitosan samples	Origin	Deacetylation degree (%)	Viscosity at 25°C (mPa s)[a]
S124	Squid	97	1750
C223	Shrimp	89	750
C232	Shrimp	87	430

[a]1% w/w chitosan in 1% w/w acetic acid solution.

the molecular weight of chitosan influence the physicochemical properties of the materials.[14,15] This biopolymer is characterized by a strong affinity for transition metals[16,17] and its ability to be cast in the form of gel beads,[18,19] fibers,[20–23] membranes,[24–26] or scaffolds.[27–29] Thus, chitosan has excellent characteristic to be used as a support for heterogeneous catalysis.[27,30–38]

We report herein for the first time the elaboration of highly porous catalytic materials based on an ionic liquid layer-containing palladium supported on chitosan. These catalytic materials have been evaluated on the hydrogenation of 4-NA into *p*-phenylenediamine in the presence of formic acid as the hydrogen donor as a model reaction. Different parameters for the elaboration process of the materials, such as the origin and concentration of chitosan and the nature of the ionic liquid, were evaluated through their impact on metal-sorption capacities, on the structure of the materials, and on their catalytic activity.

The first part of this work focuses on the elaboration of chitosan-supported ionic liquid materials in the form of HPMs. In a second part, the materials are characterized by palladium sorption studies, by the amount of palladium immobilized in the materials, and by scanning electron microscopy–energy-dispersive X-ray (SEM–EDX) analyses that enable to identify the distribution of elements within the materials, the morphology of the materials, and their mechanical resistance to compression (nonstandardized test). Finally, the catalytic properties of the materials are reported for the hydrogenation of 4-NA.

EXPERIMENTAL

Materials

Three different chitosan samples supplied by Mahtani Chitosan Pvt. (Veraval, India), named S124, C223, and C232, were used for the elaboration of the catalytic materials. The three chitosan samples originated from different sources: S124 sample was extracted from squid, while C223 and C232 samples were extracted from shrimp (Table I). Their respective deacetylation degrees were 97%, 89%, and 87%. Their viscosities (1% w/w chitosan in 1% w/w acetic acid solution) at 25°C were 1750, 750, and 430 mPa s, respectively. Two different ionic liquids (supplied by Cytec, Canada) were used for the preparation of the catalytic materials: Cyphos IL-101 (i.e., tetradecyl(trihexyl)-phosphonium chloride) and Cyphos IL-111 (tetradecyl(trihexyl)phosphonium tetrafluoroborate). Although Cyphos IL-101 is liquid at room temperature, Cyphos IL-111 has a melting temperature close to 37°C. The ionic liquids were used as supplied (without any purification).

Other reagents were of analytical grade, and they were supplied by VWR, France (HCl), Carlo Erba, Italy (NaOH, CH_3COOH, H_2SO_4), Fluka AG, Switzerland ($PdCl_2$, silica 1–3 mm particle size, $(NaPO_3)_6$), Merck, Germany (silica 63–200-μm particle size), and J.T. Baker, France (Zn powder).

Elaboration of the Catalytic Materials

Elaboration of HPMs. A 2 or 3% w/w chitosan solution in acetic acid solution (2 or 3% w/w, respectively) was prepared. The ionic liquid was mixed with 1.5 g of silica particles with a mass ratio silica/IL of 3 or 0.5. The chitosan solution was then homogeneously mixed with the ionic liquid-impregnated silica powder to reach a final volume of 50 mL. In the case of Cyphos IL-111, it was necessary to maintain the solution at 50°C using a thermostatic bath to prevent the ionic liquid solidification. The solution was introduced into molds (plate formed of cylindrical holes of 10 mm height and 10 mm diameter) that were maintained for 1 h at −78°C. The frozen cylinders were then freeze-dried with an Alpha 1–4 LD freeze dryer (Christ, Sigma).

The chitosan-supported ionic liquid HPMs were then removed from the molds and dropped in a crosslinking solution of sodium hexametaphosphate at 50 g L^{-1} (pH 6) for 12 h. At the beginning of the crosslinking process, the materials were placed under vacuum to remove air bubbles from the HPMs and improve the dispersion of sodium hexametaphosphate inside the materials. Finally, the materials were washed with water and dried at room temperature.

Table II reports the experimental conditions used for the elaboration of the different chitosan-supported ionic liquid HPMs.

Metal Immobilization. The sorption of palladium in the chitosan-supported ionic liquid materials was operated by leaving the materials for 2 days in a 150 ppm solution of palladium chloride at pH 1 (controlled with HCl solution) under soft agitation (120 rpm). The reduction of the palladium immobilized in the materials was operated by *in situ* produced hydrogen: the Pd(II)-materials were immersed in a 0.5M H_2SO_4 solution in

Table II. Conditions for the Elaboration of Chitosan-Supported Ionic Liquid Materials

Material	IL	Silica particle size	Si/IL	Chitosan (%)	Chitosan origin/DD[a] (%)
C1	111	63-200 μm	3	2	Squid/97
C2	101	63-200 μm	3	2	Squid/97
C3[b]	101	1-3 mm	3	2	Squid/97
C4	101	63-200 μm	3	2	Shrimp/89
C5	101	63-200 μm	3	2	Shrimp/87
C6[c]	111	63-200 μm	0.5	2	Squid/97
C7[d]	111	63-200 μm	3	3	Squid/97

Type of IL: Cyphos IL-101 (tetradecyl(trihexyl)phosphonium chloride) or Cyphos IL-111 (tetradecyl(trihexyl)phosphonium tetrafluoroborate).
[a]Deacetylation degree.
[b]Large silica particles are ineffective for homogeneous molding.
[c]Poor stability in water.
[d]Poor mechanical resistance to compression.

the presence of zinc powder for 3 days at 30°C under agitation to allow a complete palladium reduction. These reduction conditions were determined previously.[39] Previous studies showed that in these conditions, the metal was completely reduced (the yield ranged between 50 and 70%).[21,39] The Pd(0) materials were washed with water and dried at room temperature.

Characterization of Catalytic Materials

The amount of palladium immobilized in the catalytic materials was determined by mineralization of the materials (in triplicate)[10] followed by Pd analyses with an ICP–AES spectrophotometer (inductively coupled plasma with atomic emission spectrometer) Jobin-Yvon Activa-M (Jobin-Yvon, Longjumeau, France). The amount of ionic liquid immobilized in the catalytic materials could not be determined with this method as the phosphorus element, commonly used as a tracer of Cyphos IL-101 and 111 cations,[10] was also present as the crosslinker (sodium hexametaphosphate) of the materials.

The free volume of the catalytic materials was determined using a pycnometer. The void volume of the chitosan-supported IL and Pd materials was close to 70%.

The morphology and the distribution of ionic liquid and palladium in the materials were determined with an Environmental Scanning Electron Microscope Quanta FEG 200, equipped with an OXFORD Inca 350 Energy-Dispersive X-ray microanalysis system (SEM–EDX). SEM observations were performed on the cross-section of the catalytic materials (obtained by cutting with a thin-slice cutter). The use of environmental SEM allowed the direct observation of materials, without previous metallization of the samples. The topography of the samples was observed using secondary electron flux while the backscattered electrons were used for the identification and localization of heavy metals at the surface of the materials (by phase contrast). SEM–EDX facilities were used for the analysis of specific zones at the surface of the catalytic materials.

A mechanical test (resistance to compression) was performed using the facilities of the SEM equipped with a mechanical testing unit (Benco symmetrical bench) on a catalytic material (10 mm height and diameter). The material, fixed inside the SEM, was submitted to a compression test. The SEM facilities allowed to follow the force measured on the sensors, and the mechanical degradation of the material submitted to a 5.3 kN compression strength. A video reporting a series of microphotograph of the compression area could be recorded (available from the authors).

Catalytic Reaction

The catalytic activity of the materials was studied on the hydrogenation of 4-NA to *p*-phenylenediamine in the presence of formic acid as the hydrogen donor. During the reaction, formic acid leads to carbon dioxide and hydrogen gas where H_2 can react with the substrate through the catalyst. This simple test reaction was used to compare the catalytic efficiency of the different materials using the optimized reaction conditions obtained in a previous study.[10] Twenty-five milliliters of a solution of 4-NA (25 mg L^{-1}) were prepared. About 0.5 mL of formic acid (99% w/w) was added to the substrate solution under agitation using a magnetic stirrer. The temperature of the reactor was maintained at 25°C during the experiment by a temperature-controlled box. The catalytic material was immobilized in a column, blocked by inert synthetic foam (Figure S1, Supporting Information). The column was fed by a peristaltic pump, and the solution was continuously recirculated through column at the flow rate of 15 mL min^{-1}. An auxiliary recirculation loop was used for the analysis of the solution: the solution was circulated at the flow rate of 12 mL min^{-1} through a circulating cuvette to measure online the absorbance of the solution at 381 nm with a Shimadzu UV-1650PC spectrophotometer. The measurement of the absorbance at 381 nm allowed to evaluate the concentration of 4-NA.

The catalytic efficiencies of the different materials were compared using four parameters: (a) the conversion yield, (b) the initial rate of the reaction, (c) the half-reaction time (HRT), and (d) the turnover frequency (TOF). The conversion yield was measured at complete conversion or after a contact time of 60 min. The initial rate of the reaction was measured on the initial linear part of the kinetic curves (calculated for each reaction). The HRT corresponded to the time of reaction required to achieve half of the conversion obtained at 60 min. The TOF was measured at the HRT defined as the number of moles of substrate converted per mole of Pd and per minute.

RESULTS AND DISCUSSION

Elaboration of the Catalytic Materials

Chitosan-supported ionic liquid and palladium materials were elaborated in the form of HPMs. The poor compatibility of ionic liquid and biopolymer solutions during the encapsulation requires the use of a compatibilizing agent. Silica particles were used to improve the contact between the two phases: the ionic liquid was first impregnated onto silica particles and then mixed with the chitosan solution to obtain a stable suspension. The impregnation of ionic liquid on silica particles was studied by varying the size of silica particles and the silica/ionic liquid mass ratio in the catalytic material. Moreover, the presence of silica particles allowed air drying of the chitosan-supported ionic liquid and Pd materials without the collapse of HPM structure. To obtain stable materials, the chitosan-supported ionic liquid HPMs were crosslinked with sodium hexametaphosphate.[40]

Palladium was immobilized in the chitosan-supported ionic liquid materials by Pd(II) sorption via a palladium chloride solution, followed by a reduction step to Pd(0) by *in situ* produced hydrogen. The reduction of palladium is characterized by the color of the cross-section of the material, which is orange when the reduction step is not completely achieved and black when Pd(II) is completely reduced to Pd(0) (Figure S2, Supporting Information). The complete palladium reduction was obtained after 3 days.

Characterization of the Materials

Materials with Low Stability. Different catalytic materials were prepared by varying the type and concentration of chitosan, the nature of the ionic liquid, and the size and concentration of silica particles (Table II). Among these materials, two samples

Table III. Amount of Pd in Selected Catalytic Materials

Material	Pd amount (mg Pd g^{-1})
C1	17.2
C2	19.4
C3	19.5
C4	18.7
C5	16.9

(**C6** and **C7**) showed poor stability in water (disintegrating after 24 h) or poor mechanical resistance. The catalytic material prepared with the silica/ionic liquid mass ratio (Si/IL) of 0.5 (**C6** sample) disintegrates in water after 24 h, contrary to standard samples (**C1–C5**) prepared with the Si/IL ratio of 3. The Si/IL ratio of 3 should thus be considered as a suitable silica concentration for the elaboration of catalytic materials. The elaboration of catalytic material with a chitosan concentration of 3% (**C7** sample) instead of 2% in standard samples (**C1–C5** samples) led to materials with poor mechanical resistance. Therefore, a biopolymer solution of 2% was more appropriate to prepare the catalytic materials. The poor stability in water of **C6** sample and the poor mechanical resistance of **C7** sample did not allow their use for catalytic reaction (Table II).

In the case of the catalytic material prepared with large silica particles (**C3** sample with silica particle size of 1–3 mm), sedimentation and a phase separation of the emulsion were observed (Table II). This defect led to poorly homogeneous HPMs.

Pd(II) Sorption Properties

Palladium sorption studies were carried out in order to evaluate the influence of the type of chitosan and ionic liquid on Pd(II) sorption capacities of the chitosan-supported IL materials. Indeed, these parameters are known to have a significant influence on metal-sorption capacities.[15,41,42] The uptake kinetics of Pd(II) sorption was compared for **C2** and **C4** materials that were prepared with chitosan issued from squid and shrimp, with a deacetylation degree of 97 and 89%, respectively. Similar Pd(II) uptake kinetics were obtained for both samples, requiring about 20 h to reach the equilibrium (Figure S3, Supporting Information), showing the low influence of the origin of chitosan and its deacetylation degree. The influence of the type of chitosan in the materials was also evaluated on Pd(II) sorption isotherms, by comparing **C2**, **C4**, and **C5** samples, which have deacetylation degrees of 97, 89, and 87%, respectively. The three materials presented similar Pd(II) sorption isotherms with maximum metal uptakes about 22–27 mg Pd g^{-1} (Figure S4, Supporting Information). The Pd(II) sorption isotherms were also compared for **C1** and **C2** samples that were prepared with different ionic liquids: Cyphos IL-111 in **C1** sample and Cyphos IL-101 in **C2** sample. Sorption isotherms poorly changed between the two samples that had a maximum metal uptake of 22 mg Pd g^{-1} (Figure S4, Supporting Information). Thus, the Pd(II) sorption properties were poorly influenced by the type of chitosan or ionic liquid used for the elaboration of chitosan-supported ionic liquid materials.

Amount of Pd in the Catalytic Materials. The amount of palladium immobilized on the catalytic materials was determined by the mineralization of chitosan-supported ionic liquid and Pd materials, followed by ICP–AES analysis of the solutions. Similar amounts of palladium were immobilized in different catalytic materials (**C1–C5** samples) between 17 and 20 mg Pd g^{-1} (Table III). No significant difference was observed depending on the parameters of elaboration of the materials: the type of chitosan (**C2**, **C4**, and **C5** samples), the type of ionic liquid (**C1** and **C2** samples), or the size of silica particles (**C2** and **C3** samples). This confirms, as described in the previous section, that the parameters of elaboration of the materials did not influence their palladium-sorption properties.

Morphology of the Catalytic Materials. SEM observations were performed on the cross-section of the catalytic materials to compare the texture and the organization of material porosity (see Supporting Information Figures S5–S9). The catalytic materials presented a macroporous structure with open pores of various diameters (50–200 μm).

Silica particles were clearly identified in the chitosan network as bulky particle pieces (Figures S5–S9, Supporting Information; Figure 1). The influence of the silica particle size on the morphology of the catalytic materials was studied in comparison with **C3** sample (silica particle size of 1–3 mm; Figure S7, Supporting Information) with **C1–C2** and **C4–C5** samples (silica particle size of 63–200 μm; Figures S5–S6 and S8–S9, Supporting Information, respectively). In the case of the catalytic

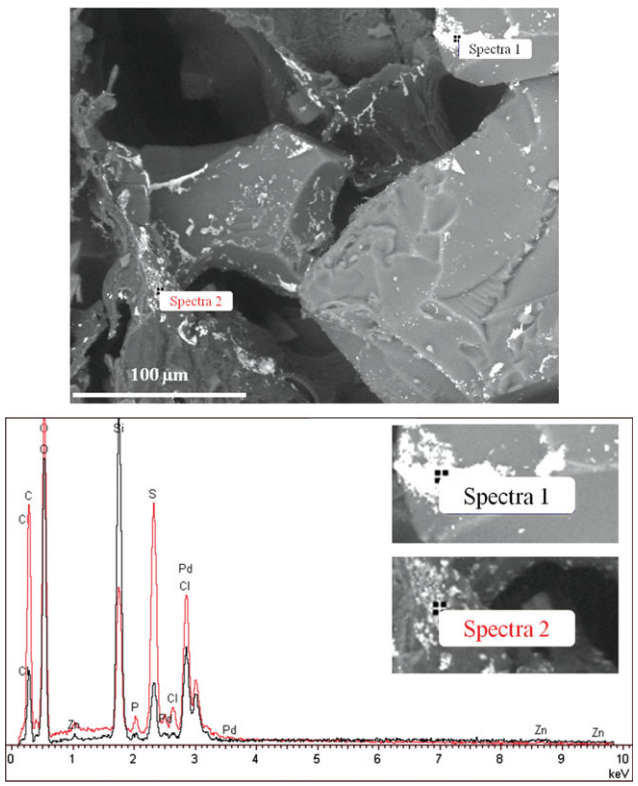

Figure 1. SEM–EDX analysis of specific zones of C1 catalytic material. [Color figure can be viewed in the online issue, which is available at wileyonlinelibrary.com.]

materials prepared with small mineral particles (**C1–C2** and **C4–C5** samples), the distribution of silica particles appeared homogeneous whereas for the largest silica particles (**C3** sample), few silica particles were observed showing the heterogeneity of the material. This is consistent with the sedimentation and the phase separation of the emulsion used for the preparation of the catalytic material containing large silica particles (**C3** sample), leading to heterogeneous catalytic materials with large pores.

The nature of the ionic liquid could have an influence on the structure of materials. Indeed, in the case of the immobilization of different ionic liquids in alginate beads, the melting properties of the ionic liquid (Cyphos IL-111, solid at room temperature, versus Cyphos IL-101, liquid at room temperature) influenced the internal porous structure of the materials.[42] Surprisingly, in this study, the nature of ionic liquid used for the preparation of the catalytic materials (Cyphos IL-111 for **C1** sample; Figure S5, Supporting Information, and Cyphos IL-101 for **C2** sample; Figure S6, Supporting Information) hardly affected the morphology of the material. No influence of the nature of ionic liquid on the porous structure of the catalytic materials was observed by SEM.

The catalytic materials were prepared with three chitosan samples, which had different deacetylation degrees (97, 89, and 87% for **C2**, **C4**, and **C5** samples, respectively). No significant change was observed by SEM in the structure of the materials. Thus, the type of chitosan used for the elaboration of the catalytic materials hardly affects the porosity of the materials.

Distribution of Elements. The observation of the SEM phase-contrast photographs (backscattered electrons) showed the presence of white aggregates, at the surface of silica particles, which corresponded to dense elements (such as Pd). Actually, silica particles were first impregnated with ionic liquid before immobilization into the chitosan matrix. Palladium was then bound to the ionic liquid through ion exchange mechanism. It was thus consistent that Pd element (dense element) appeared on the interfacial surface of the ionic liquid-silica particles. SEM–EDX analyses were performed on a catalytic material and focused on two white areas located on silica particles in order to confirm that these areas corresponded to Pd and ionic liquid impregnated in silica particles (Figure 1). As described in the previous section, no influence of the type of biopolymer or ionic liquid was observed on the structure of the catalytic material. Thus, the SEM–EDX analyses were performed on **C1** sample, representative of the catalytic materials.

The main elements observed by SEM–EDX were Si, P, Pd, Cl, S, and Zn (Figure 1). The absorption of ionic liquid (P as a tracer of the ionic liquid cation) in the porosity of the silica particles and the reaction of Pd(II) chloroanionic species with the ionic liquid[43] may explain the localization of P, Si, and Pd elements in the white aggregates on the photographs. Cl was generally related to tetrachloropalladate anions that were bound to the ionic liquid during metal adsorption. An incomplete metal reduction might explain the presence of chloride element in the catalytic material. The presence of S and Zn elements can be respectively attributed to sulfuric acid and Zn powder used for the *in situ* production of hydrogen for Pd(II) reduction. The SEM–EDX analyses confirmed that palladium and ionic liquid were located on silica particles, within the chitosan matrix. Pd particles were generally aggregated showing a heterogeneous distribution, as seen in Figures S5–S9 (Supporting Information).

Mechanical Properties. The catalytic materials were designed for dynamic applications in flow column reaction. With increasing the flow rate of the reaction, the catalytic materials are submitted to compression. To evaluate their mechanical resistance, a compression study was made using the SEM-Benco bench facilities. This procedure was not normalized and only allowed to approach mechanical characteristics. The mechanical test was performed on **C2** sample, representative of other catalytic materials. Selected SEM pictures corresponding to different phases of the compression test are presented together with the mechanical test in Figure S10 (Supporting Information).

The compression test allowed obtaining a graph representing the strength (in N) as a function of the compression length (in mm). The profile corresponding to **C2** sample presented first a linear increase of the compression length with the strength (step 1). Then a plateau was observed: the compression length increased while the strength remained stable (steps 2–4). Finally, the rupture of the material occurred when the strength increased and exceeded 100 N. For a comparison, in the case of alginate-based catalytic materials without mechanical strengthener, the rupture of the material occurred with a strength of 40 N, while alginate-based catalytic materials containing cellulose fibers as mechanical strengthener could undergo strength of 1750 N.[13]

The different selected SEM pictures illustrate the deformation of the material under compression: a V-shaped crack formed in the higher part of the material (step 2) and progressively propagate (till step 4) before the rupture of the material could be identified (step 5). The compression test was followed by the expulsion of silica particles in the microscope cell. This means that silica particles were not tightly bound to the biopolymer network (at least a significant part of the mineral loaded). This was consistent with the SEM observations that clearly showed that the silica particles isolated from the biopolymer matrix. The weak interaction of these mineral particles with the chitosan network might cause substantial decrease of mechanical resistance to compression.

However, the compression force applied on the materials was far more important for the mechanical test than during its use in catalysis. Thus, the catalytic material had enough mechanical resistance to compression to be used in column reactor with a flow rate of 15 mL min^{-1} (corresponding to the experimental conditions selected for the present study).

Catalytic Properties of the Materials

The catalytic properties of the materials were studied for **C1–C5** samples, because **C6** sample was not stable in water and **C7** sample had poor mechanical stability. The catalytic properties of chitosan-supported ionic liquid and Pd materials were evaluated on a model reaction, the hydrogenation of 4-NA into *p*-phenylenediamine in the presence of formic acid as hydrogen

Applied Polymer SCIENCE

Table IV. Catalytic Properties of Selected Catalytic Materials

Material	Conversion yield (%)[a]	Linear time (min)	Initial rate (min^{-1})	Half-reaction time (min)	TOF @ HRT (mol 4-NA mol^{-1} Pd min^{-1})
C1	100	7	0.35	2	0.20
C2	90	5	0.07	16	0.38
C3	100	5	0.29	3.5	0.18
C4	100	8	0.38	1.5	0.19
C5	100	10	0.29	2.1	0.23

[a]After a reaction time of 60 min.

donor. Four parameters were measured to evaluate the activity of the catalytic materials: (a) the conversion yield, (b) the initial rate of the reaction, (c) the HRT, and (d) the TOF. The conversion yield was measured at complete conversion or after a contact time of 60 min (this reaction time was long enough to reach complete conversion for most catalytic materials). The initial rate of the reaction was measured on the initial linear part of the kinetic curves (calculated for each reaction). The HRT corresponded to the time of reaction required to achieve half of the conversion obtained at 60 min. The TOF was measured at the HRT defined as the number of moles of substrate converted per mole of Pd and per minute. Table IV reports the values of these catalytic parameters for the different catalytic materials. It is noteworthy that no leaching of Pd on the outlet solutions was observed by ICP–AES analyses, which confirmed the stability of the catalytic materials tested.

Influence of the Ionic Liquid. Two ionic liquids were immobilized on the catalytic materials: Cyphos IL-111 (solid at room temperature) in **C1** sample and Cyphos IL-101 (liquid at room temperature) in **C2** sample. The 4-NA hydrogenation was strongly affected by the type of ionic liquid immobilized in the catalytic materials (Figure 2 and Table IV). In the case of the catalytic material prepared with Cyphos IL-101 (**C2** sample), a high-TOF was obtained (0.38 mol 4-NA mol^{-1} Pd min^{-1}), but with a low-reaction kinetic (initial rate of 0.07 min^{-1} and half reaction time of 16 min). Indeed, with this catalytic material, even after 60 min of reaction, the 4-NA hydrogenation was not

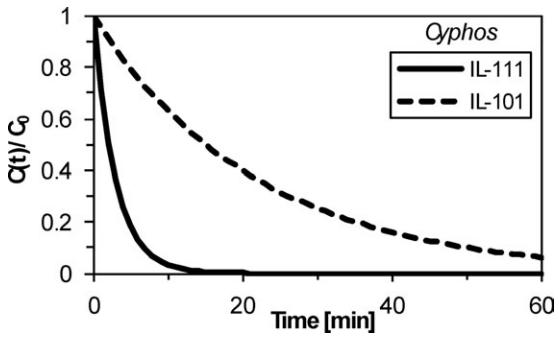

Figure 2. Impact of the type of ionic liquid on the catalytic hydrogenation of 4-NA [catalytic materials: C1 (Cyphos IL-111) and C2 (Cyphos IL-101)].

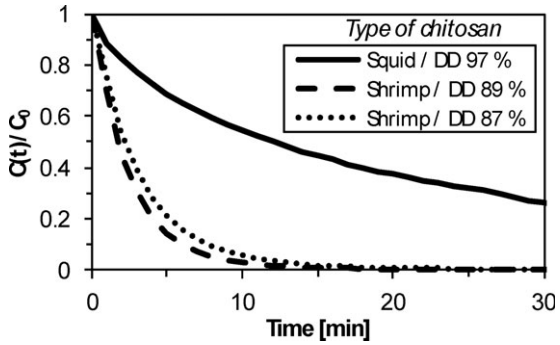

Figure 3. Impact of the type of chitosan (origin and deacetylation degree) on the catalytic hydrogenation of 4-NA [catalytic materials: C2 (Squid/DD 97%), C4 (Shrimp/DD 89%), and C5 (Shrimp/DD 87%)].

complete (90% conversion obtained). On the contrary, the catalytic material prepared with Cyphos IL-111 (**C1** sample) led to a lower TOF (0.20 mol 4-NA mol^{-1} Pd min^{-1}), but a much higher reaction kinetic (initial rate of 0.35 min^{-1} and half reaction time of 2 min) and a complete conversion of the substrate was achieved in 15–20 min.

The higher reaction rate obtained with the catalytic material containing Cyphos IL-111 (**C1** sample) might be explained by the characteristic of this ionic liquid. Indeed, in the elaboration of the catalytic materials, the ionic liquids were first impregnated onto silica particles. In the case of the ionic liquid Cyphos IL-111, which is solid at the experimental temperature (25°C), we assume that the ionic liquid might be immobilized only at the outer layers of the mineral support. This would make the ionic liquid, and thus the palladium bound to the ionic liquid, more accessible for the diffusion of substrate molecules in the catalytic material.

Influence of the Type of Chitosan. Three types of chitosan, from different sources and with different deacetylation degrees, were used for the elaboration of the catalytic materials (**C2**, **C4**, and **C5** samples with deacetylation degrees of 97, 89, and 87%, respectively). The comparison of the hydrogenation kinetics for the catalytic materials prepared with different types of chitosan showed that the properties of the biopolymer had an influence on the reaction rate (Figure 3 and Table IV). When using the catalytic materials prepared with the two chitosan of lower deacetylation degree (**C4** and **C5** samples), the complete conversion of the substrate was achieved in 15 min (for **C4** and **C5** samples, initial rates of 0.38 and 0.29 min^{-1}, respectively, and half reaction times of 1.5 and 2.1 min, respectively). In the case of the catalytic material containing the chitosan of higher deacetylation degree (**C2** sample), a significant decrease in the reaction rate was observed with an initial rate of 0.07 min^{-1} and a half reaction time of 16 min. However, the material prepared with the chitosan of higher deacetylation degree led to a higher TOF (0.38 mol 4-NA mol^{-1} Pd min^{-1} for **C2** sample) than the materials prepared with the two chitosan samples having the lower deacetylation degrees (0.19 mol 4-NA mol^{-1} Pd min^{-1} and 0.23 mol 4-NA mol^{-1} Pd min^{-1} for **C4** and **C5** samples, respectively).

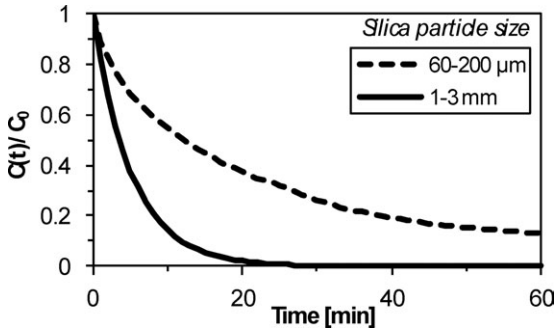

Figure 4. Impact of the silica particle size on the catalytic hydrogenation of 4-NA [catalytic materials: C2 (60–200 μm) and C3 (1–3 mm)].

The properties of the chitosan (deacetylation degree and viscosity) used for the elaboration of the catalytic materials might affect the accessibility and availability of catalytic species. In previous studies, it had been reported that the origin of the material and its structural properties could influence the sorption of precious metal anions on chitosan.[15,41] The characteristics of the chitosan might thus be carefully controlled to insure a good reproducibility for the wide spreading of chitosan-based materials.

Influence of the Silica Particles Size. Two catalytic materials were prepared with either small silica particles (60–200-μm particle size in **C2** sample) or large silica particles (1–3 mm for **C3** sample). Even if the material prepared with large particle size (**C3** sample) presented low homogeneity in structure (see previous sections), its catalytic efficiency could be evaluated (Figure 4 and Table IV). The reaction kinetic was higher with the catalytic material prepared with large silica particles (initial rate of 0.29 min^{-1} and half reaction time of 3.5 min for **C3** sample) than those prepared with small silica particles (initial rate of 0.07 min^{-1} and half reaction time of 16 min for **C2** sample). However, a higher catalytic efficiency is obtained with the material containing small silica particles (TOF 0.38 mol 4-NA mol^{-1} Pd min^{-1} for **C2** sample) than with the material prepared with large silica particles (TOF 0.18 mol 4-NA mol^{-1} Pd min^{-1} for **C3** sample). Nevertheless, even if the use of large silica particles in the catalytic materials led to materials with satisfactory catalytic efficiency, the low homogeneity of the material and its low-mechanical stability limit their use. The catalytic materials prepared with small silica particles may thus be favored.

Catalytic Efficiency of Chitosan-Supported Ionic Liquid and Pd HPMs. The catalytic materials based on chitosan-supported ionic liquid and Pd presented in this study allowed to obtain TOF from 0.19 to 0.38 mol 4-NA mol^{-1} Pd min^{-1} with 90–100% conversion yields, depending on the parameters of elaboration of the materials (type of ionic liquid, type of chitosan and silica particle size; Table IV). In similar reaction conditions, alginate-supported ionic liquid and Pd catalysts led to TOF from 0.12 to 0.43 mol 4-NA mol^{-1} Pd min^{-1} with 70–100% conversion yields, also depending on the parameters of elaboration of the materials (freezing temperature, M/G molar ratio, gelation mode, concentration of porogen agent, and presence of cellulose fibers).[13] Thus the elaboration of biopolymer-supported ionic liquid and Pd catalysts in the form of HPMs with alginates or chitosan led to similar catalytic efficiency for the hydrogenation of 4-NA in column reactor. In the case of chitosan-supported ionic liquid and Pd materials, higher catalytic performances were obtained with the catalysts prepared with chitosan of high-deacetylation degree and with the ionic liquid Cyphos IL-101. These catalytic performances can tentatively be compared to those of other supports. Vincent et al.[30] investigated the hydrogenation of 4-NA with palladium immobilized on chitosan particles. The kinetic profiles appeared to be similar to the present profiles (except for the optimum conditions identified in this work that were slightly more favorable, as shown by the shorter reaction time required for achieving the complete conversion of the substrate). However, the experimental conditions being different, the direct comparison is made difficult. Alexander et al.[44] investigated the hydrogenation of 4-NA in a series of organic solvents using Pd(II) immobilized on a polymer bearing Schiff base groups and hydrogen gas as the hydrogen donor. The comparison of experimental results (type and concentration of hydrogen donor, catalyst load, substrate concentration…) with the present data is then difficult; however, the TON varied with the substrate between 2 and 30, which is of the same order of magnitude than the values found in the present work.

CONCLUSIONS

Chitosan was efficiently used, combined with silica particles, to immobilize phosphonium-based ionic liquids and to elaborate materials in the form of HPMs. Pd(II) sorption on these HPMs followed by metal reduction led to chitosan-palladium and ionic liquid composite catalysts. These materials proved to be efficient catalysts for 4-NA hydrogenation in the presence of formic acid as the hydrogen donor, in column reactor.

The metal sorption on chitosan-supported ionic liquid materials was not influenced by the experimental conditions used for the elaboration of the materials, with similar Pd(II) uptake kinetics and sorption isotherms. The amount of palladium efficiently immobilized on the materials was about 17–20 mg Pd g^{-1}. SEM–EDX analyses showed that the palladium catalyst was loaded in the ionic liquid, immobilized on silica particles, and dispersed in the chitosan matrix.

The type of chitosan used for the elaboration of the catalytic materials (source of biopolymer and degree of deacetylation) did not significantly change the structure of the materials, but affected their catalytic efficiency. The higher TOF was obtained with the chitosan of higher deacetylation degree (extracted from squid). However, chitosan with lower deacetylation degree (from shrimp) also presented good catalytic activity. The use of a high-chitosan concentration led to a poor mechanical stability of the material, which could not be used for catalytic reaction. A biopolymer solution of 2% w/w should thus be considered as a suitable concentration for the elaboration of the catalytic materials.

Surprisingly, no change in the porous structure of the materials was observed using two different ionic liquids (Cyphos IL-111

and Cyphos IL-101). The TOF was higher in the case of the materials prepared with Cyphos IL-101 than with Cyphos IL-111, although slower reaction rate was obtained.

Silica particles were included in the catalytic material to enable the immobilization of the hydrophobic ionic liquid in the chitosan aqueous solution. When the concentration of silica particles was too low, the materials were not stable in water, preventing their use as catalytic materials. The Si/IL ratio of 3 should thus be considered as a suitable silica concentration for the elaboration of the catalytic materials. The size of silica particles was also a significant parameter: only small mineral particles (63–200 μm) led to homogeneous material.

Finally, optimum conditions in terms of mechanical stability and catalytic activity are a catalytic material made of chitosan with a high-deacetylation degree, at a concentration of 2% w/w in solution, using small silica particles and Cyphos IL-101, with a Si/IL mass ratio of 3.

These promising results open the way for the elaboration of catalytic materials based on biopolymer to immobilize various ionic liquids and transition metal catalysts. The method used in the study might be applied to the design of SILCs in the form of HPMs. The resultant catalytic materials should allow applications in fixed-bed reactors for continuous flow catalysis in liquid or gas phase.

ACKNOWLEDGMENTS

The financial support from Agence Nationale de la Recherche to the BiopSIL project (ANR-08-CP2D-02) is greatly acknowledged. Authors thank Jean-Marie TAULEMESSE (from Centre des Matériaux de Grande Diffusion at Ecole des Mines d'Alès) for SEM and SEM–EDX facilities.

REFERENCES

1. Riisager, A.; Fehrmann, R.; Haumann, M.; Wasserscheid, P. *Eur. J. Inorg. Chem.* **2006,** *44*, 695.
2. Wasserscheid, P. *J. Indus. Eng. Chem.* **2007,** *13*, 325.
3. Zhang, Q. H.; Zhang, S. G.; Deng, Y. Q. *Green Chem.* **2011,** *13*, 2619.
4. Gu, Y. L.; Ogawa, C.; Kobayashi, J.; Mori, Y.; Kobayashi, S. *Angew. Chem. Int. Ed.* **2006,** *45*, 7217.
5. Mehnert, C. P. *Chem. A Eur J* **2005,** *11*, 50.
6. Riisager, A.; Eriksen, K. M.; Wasserscheid, P.; Fehrmann, R. *Catal. Lett.* **2003,** *90*, 149.
7. Moucel, R.; Perrigaud, K.; Goupil, J. M.; Madec, P. J.; Marinel, S.; Guibal, E.; Gaumont, A. C.; Dez, I. *Adv. Synth. Catal.* **2010,** *352*, 433.
8. Clousier, N.; Moucel, R.; Naik, P.; Madec, P. J.; Gaumont, A. C.; Dez, I. *Comptes Rendus Chim.* **2011,** *14*, 680.
9. Baudoux, J.; Perrigaud, K.; Madec, P. J.; Gaumont, A. C.; Dez, I. *Green Chem.* **2007,** *9*, 1346.
10. Jouannin, C.; Dez, I.; Gaumont, A. C.; Taulemesse, J. M.; Vincent, T.; Guibal, E. *Appl. Catal. B: Environ.* **2011,** *103*, 444.
11. Quignard, F.; Di Renzo, F.; Guibal, E. *Topics in Current Chemistry* **2010**, *294*, 165.
12. Valentin, R.; Molvinger, K.; Viton, C.; Domard, A.; Quignard, F. *Biomacromolecules* **2005,** *6*, 2785.
13. Jouannin, C.; Vincent, C.; Dez, I.; Gaumont, A.-C.; Vincent, T.; Guibal, E. *Nanomaterials* **2012,** *2*, 31.
14. Quignard, F.; Valentin, R.; Di Renzo, F. *New J. Chem.* **2008,** *32*, 1300.
15. Jaworska, M.; Sakurai, K.; Gaudon, P.; Guibal, E. *Polym. Int.* **2003,** *52*, 198.
16. Guibal, E. *Separ. Purif. Technol.* **2004,** *38*, 43.
17. Rhazi, M.; Desbrieres, J.; Tolaimate, A.; Rinaudo, M.; Vottero, P.; Alagui, A.; El Meray, M. *Eur. Polym. J.* **2002,** *38*, 1523.
18. Ngah, W. S. W.; Endud, C. S.; Mayanar, R. *React. Funct. Polym.* **2002,** *50*, 181.
19. Ngah, W. S. W.; Ab Ghani, S.; Kamari, A. *Bioresour. Technol.* **2005,** *96*, 443.
20. Desai, K.; Kit, K.; Li, J.; Zivanovic, S. *Biomacromolecules* **2008,** *9*, 1000.
21. Peirano, F.; Vincent, T.; Quignard, F.; Robitzer, M.; Guibal, E. *J. Membr. Sci.* **2009,** *329*, 30.
22. Liu, C. X.; Bai, R. B. *J. Membr. Sci.* **2006,** *284*, 313.
23. Qian, L.; Zhang, H. F. *Green Chem.* **2010,** *12*, 1207.
24. Vieira, R. S.; Guibal, E.; Silva, E. A.; Beppu, M. M. *Adsorp.-J. Int. Adsorp. Soc.* **2007,** *13*, 603.
25. Krajewska, B. *Separ. Purif. Technol.* **2005,** *41*, 305.
26. Fernandes, S. C. M.; Oliveira, L.; Freire, C. S. R.; Silvestre, A. J. D.; Neto, C. P.; Gandini, A.; Desbrieres, J. *Green Chem.* **2009,** *11*, 2023.
27. Hortiguela, M. J.; Aranaz, I.; Gutierrez, M. C.; Ferrer, M. L.; del Monte, F. *Biomacromolecules* **2011,** *12*, 179.
28. Madihally, S. V.; Matthew, H. W. T. *Biomaterials* **1999,** *20*, 1133.
29. Rinki, K.; Tripathi, S.; Dutta, P. K.; Dutta, J.; Hunt, A. J.; Macquarrie, D. J.; Clark, J. H. *J. Mater. Chem.* **2009,** *19*, 8651.
30. Vincent, T.; Peirano, F.; Guibal, E. *J. Appl. Polym. Sci.* **2004,** *94*, 1634.
31. Guibal, E. *Prog. Polym. Sci.* **2005,** *30*, 71.
32. Leonhardt, S. E. S.; Stolle, A.; Ondruschka, B.; Cravotto, G.; De Leo, C.; Jandt, K. D.; Keller, T. F. *Appl. Catal. A-Gen.* **2010,** *379*, 30.
33. Chtchigrovsky, M.; Primo, A.; Gonzalez, P.; Molvinger, K.; Robitzer, M.; Quignard, F.; Taran, F. *Angew. Chem. Int. Ed.* **2009,** *48*, 5916.
34. Macquarrie, D. J.; Hardy, J. J. E. *Indus. Eng. Chem. Res.* **2005,** *44*, 8499.
35. Corma, A.; Concepcion, P.; Dominguez, I.; Fornes, V.; Sabater, M. J. *J. Catal.* **2007,** *251*, 39.
36. Alesi, S.; Di Maria, F.; Melucci, M.; Macquarrie, D. J.; Luque, R.; Barbarella, G. *Green Chem.* **2008,** *10*, 517.

37. Yi, S. S.; Lee, D. H.; Sin, E.; Lee, Y. S. *Tetrahedron Lett.* **2007,** *48*, 6771.
38. Huang, A. M.; Liu, Y. F.; Chen, L.; Hua, J. D. *J. Appl. Polym. Sci.* **2002,** *85*, 989.
39. Vincent, T.; Guibal, E. *Indus. Eng. Chem. Res.* **2002,** *41*, 5158.
40. Sicupira, D.; Campos, K.; Vincent, T.; Leao, V.; Guibal, E. *Adsorp. J. Int. Adsorp. Soc.* **2010,** *16*, 127.
41. Jaworska, M.; Kula, K.; Chassary, P.; Guibal, E. *Polym. Int.* **2003,** *52*, 206.
42. Guibal, E.; Pinol, A. F.; Ruiz, M.; Vincent, T.; Jouannin, C.; Sastre, A. M. *Separ. Sci. Technol.* **2010,** *45*, 1935.
43. Vincent, T.; Parodi, A.; Guibal, E. *React. Funct. Polym.* **2008,** *68*, 1159.
44. Alexander, S.; Udayakumar, V.; Nagaraju, N.; Gayathri, V. *Transit. Metal Chem.* **2010,** *35*, 247.